Spectral compression in a multipass cell

Nour Daher, Florent Guichard, Xavier Délen, Yoann Zaouter, Marc Hanna, Patrick Georges

Research Article | Vol. 28, No. 15 / 20 July 2020 / Optics Express 21571
Optics EXPRESS

Spectral compression in a multipass cell

NOUR DAHER,[1,*] FLORENT GUICHARD,[2] XAVIER DÉLEN,[1] YOANN ZAOUTER,[2] MARC HANNA,[1] AND PATRICK GEORGES[1]

[1]Université Paris-Saclay, Institut d'Optique Graduate School, CNRS, Laboratoire Charles Fabry, 91127 Palaiseau, France
[2]Amplitude Laser, 11 Avenue de Canteranne, Cité de la Photonique, 33600 Pessac, France
[*]nour.daher@institutoptique.fr

Abstract: Starting from a femtosecond ytterbium-doped fiber amplifier, we demonstrate the generation of near Fourier transform-limited high peak power picosecond pulses through spectral compression in a nonlinear solid-state-based multipass cell. Input 260 fs pulses negatively chirped to 2.4 ps are spectrally compressed from 6 nm down to 1.1 nm, with an output energy of 13.5 μJ and near transform-limited pulses of 2.1 ps. A pulse shaper included in the femtosecond source provides some control over the output spectral shape, in particular its symmetry. The spatial quality and spatio-spectral homogeneity are conserved in this process. These results show that the use of multipass cells allows energy scaling of spectral compression setups while maintaining the spatial properties of the laser beam.

1. Introduction

Spectral compression of negatively chirped pulses in a nonlinear medium is an elegant way to turn a femtosecond laser source into a close to Fourier transform-limited (FTL) picosecond source [1]. This allows the design of synchronized sources with widely different durations, of particular importance for a variety of nonlinear spectroscopy experiments such as stimulated Raman scattering microscopy [2]. Powerful laser sources delivering few picosecond UV pulses are also required in free electron laser installations to trigger the photocathode [3], and can be obtained by frequency converting FTL ps pulses in the near infrared. Starting from a femtosecond laser, self-phase modulation can be used to generate both picosecond sources through spectral compression [4] and a few-cycle beam through temporal compression [5]. Spectral compression can be intuitively understood as follows: an initial negative frequency chirp is compensated by the frequency shift induced by self-phase modulation. This frequency shift, in turn, is determined by the temporal intensity profile, which itself is related to the spectral profile since the pulses are chirped.

Most spectral compression experiments have been performed in single transverse mode solid-core optical fibers [1,4,6–9], that allow to increase the interaction length almost arbitrarily, and fix the spatial profile. As a consequence, the pulse energy is limited by the damage threshold at the fiber facet and catastrophic self-focusing if the peak power exceeds the critical power in fused silica. This corresponds to energies of 1–10 μJ for pulses in the 1–10 ps duration range. Although it has never been done to our knowledge, gas-filled capillaries could in principle be used to perform spectral compression, but their losses typically restricts their use to pulse energies above 1 mJ for picosecond pulses. This gap in pulse energy could in principle be filled by use of gas-filled Kagome or anti-resonant microstructured hollow-core fibers, but no demonstration was reported. An alternative technique for energy scaling is possible using hybrid architectures, where nonlinearities are distributed over fiber and bulk amplifiers [10]. A few experiments [11,12] have also reported the observation of spectral compression in bulk media for pulses with much higher energies (mJ level), with moderate spectral compression factors. In this case, the complex

#397191 https://doi.org/10.1364/OE.397191
Journal © 2020 Received 8 May 2020; revised 26 Jun 2020; accepted 26 Jun 2020; published 7 Jul 2020

Optics EXPRESS

spatio-temporal dynamics induces spatio-spectral couplings, which limits the applicability of the method.

Recently, multipass cells (MPC) have been proposed and used as a platform to perform nonlinear optics at high pulse energies while essentially retaining the one dimensional dynamics that is observed in optical fibers. A solid or gas nonlinear medium is inserted inside the cell, allowing easy tuning of the nonlinearity level through the gas pressure or bulk medium thickness, while dispersion properties may be easily tailored through appropriate mirrors coatings. This concept has been used mostly to implement temporal compression in a wide range of pulse energies and durations [13–17]. In the case of experiments that make use of a bulk medium inserted in the MPC the peak power scaling is not limited by the critical power because the pulses exit the nonlinear medium before catastrophic collapse at each pass. MPCs are therefore a valid alternative to solid- or hollow-core fibers and capillaries as a platform for nonlinear optics, and can be advantageous in terms of transmission, possibilities in dispersion and nonlinearity engineering, and polarization-maintaining properties.

In this article, we report the use of a MPC to perform spectral compression at ~27 μJ input energy, beyond what is possible in solid core fibers. Negatively chirped pulses generated from a high-energy ytterbium-doped fiber chirped pulse amplifier (FCPA) are spectrally compressed, starting from a spectral full width at half maximum (FWHM) of 6 nm down to 1.1 nm. In the time domain, this corresponds to the generation of FTL 2.1 ps pulses. The MPC nonlinearity is provided by plates of fused silica inserted in the cell. A pulse shaper included in the fiber amplifier architecture allows us to finely adjust the negative frequency chirp and control the process in order to obtain a symmetrical spectral compression. The measured output beam quality factor is $M^2 = 1.2 \times 1.0$ with high spectral homogeneity. This proof of principle constitutes an additional example of the use of MPC to scale the energy of nonlinear subsystems that are usually implemented using optical fibers.

2. Experiment

Spectral compression is performed with the experimental setup shown in Fig. 1. The input pulses originate from a FCPA operating at a central wavelength of 1030 nm, delivering quasi-FTL 260 fs 30 μJ pulses at a repetition rate of 1 MHz. The output spectrum exhibits a nearly Gaussian shape with a FWHM of 6 nm. A commercially available pulse shaper is inserted in the laser architecture before the main amplifier to allow control over the spectral intensity and phase in this quasi-linear amplifier system, similarly to the system described in [18]. This pulse shaper is based on a spatial light modulator inserted in the Fourier plane of a 4f dispersive line, with a spectral resolution of 100 pm, and provides both intensity and phase shaping capabilities. The measured spatial quality factor of the laser beam is $M^2 = 1.1$ along both horizontal and vertical directions.

The multipass cell is a Herriot-type [19] cell and consists of two concave mirrors with 2 inches diameter facing each other with a radius of curvature of 300 mm and coated with high reflectivity, low group delay dispersion dielectric stacks on a 980-1080 nm bandwidth. Two 12 mm-thick AR-coated fused silica plates, spaced by 23 mm, are added near the center of the MPC to serve as nonlinear media. Using fused silica as a nonlinear medium allows us to introduce a higher level of nonlinearity compared to gas-filled MPCs, due to a three order of magnitude higher nonlinear refractive index $n_2 = 2.2 \times 10^{-20}$ m^2/W [20]. This does not prevent operation at peak powers well above the critical power of self-focusing of 5 MW if the self-focusing distance is greater than the plate thickness [13]. The distance between the MPC mirrors is adjusted to 554 mm. Mode-matching to the stationary MPC beam is achieved by an arrangement of three lenses, resulting in a beam diameter of 370 μm at the waist, 9% larger than the resonant waist beam diameter (assuming an M^2=1.1). The beam diameter on mirrors is 1.24 mm, leading to an energy density well below the damage threshold, thus allowing straightforward energy scaling of this

Optics EXPRESS

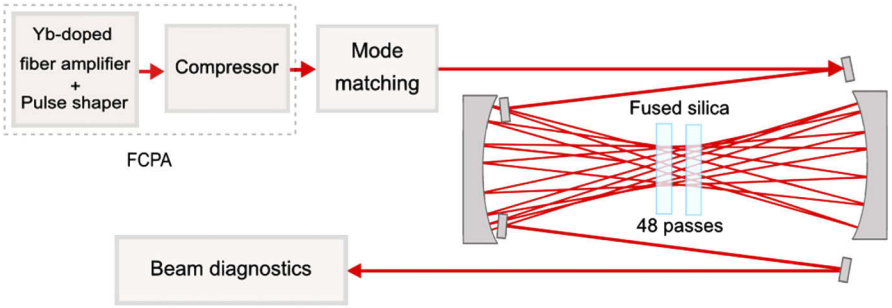

Fig. 1. Experimental setup. The high energy FCPA system includes a pulse shaper that allows modification of the output spectral phase, and the compressor can also be adjusted to modify the output pulse chirp. Mode matching is achieved by an arrangement of three lenses. After propagation in the MPC, the beam is analyzed using a FROG setup, beam profiler, M^2 measurement setup, and imaging spectrometer.

scheme. Two 3 mm width rectangular mirrors located in front of one of the MPC mirrors are used to couple the beam into and out of the cell. The number of roundtrips (reflections on each MPC mirror) in the MPC is 24.

The power transmission of the MPC is 51%, including the mode-matching optics. This low value is mostly due to the non-optimal AR coating of the fused silica plates, with an estimated reflectance higher than 0.1% for each interface. It could be readily increased using a single 24 mm plate and better quality AR coating [13,14]. The beam at the output of the MPC is collimated and characterized. The pulse temporal profile and spectrum at the output of the MPC are measured by means of a home-built second harmonic-generation frequency resolved optical gating (FROG) setup.

We start by introducing the necessary negative chirp for spectral compression by changing the distance between the gratings inside the FCPA. The pulse duration is broadened from 260 fs to 2.1 ps. In this case, Fig. 2 shows the results of an optimal spectral compression obtained at 19 µJ input energy. The spectrum FWHM is compressed from 6 nm down to 1.06 nm while the temporal duration of the negatively chirped pulse remains unchanged after spectral compression. The time-bandwidth product (TBP) of the pulse at the output of the MPC is 0.66 indicating a transform-limited pulse: the TBP of a FTL pulse exhibiting the temporal profile of the output pulse in this example is 0.64. An asymmetrical spectral shape with side lobes on the long wavelength side is observed after compression as shown in Fig. 2(d). This is also noticeable in the associated FROG traces shown in Figs. 2(a)–2(b).

As stated in the introduction, the spectral compression mechanism involves an initial negative instantaneous frequency chirp and subsequent SPM-induced frequency shift. When all relevant quantities such as instantaneous frequency, spectral, and temporal intensity profiles are symmetric with respect to a center frequency, the process leads to a symmetric spectrum. However, slight asymmetry in these shapes due to e. g. the real gain profile of the amplifier, or cubic spectral phase, lead to a non-symmetric output spectrum as observed here. In order to control the spectral compression and obtain a cleaner spectral shape at the output, we use the pulse shaper embedded in the laser architecture.

In this second experiment, starting from an optimally compressed pulse with a duration of 260 fs, the chirp is now introduced at the pulse shaper with a quadratic phase $\varphi_2 = -190\times10^3$ fs^2 and a cubic phase $\varphi_3 = -9\times10^6$ fs^3 leading to the generation of 2.4 ps pulses at the output of the FCPA. Note that chirping with the grating compressor lead to the opposite sign of third-order spectral phase, since the φ_3/φ_2 ratio is negative for gratings pairs. The results of the FROG measurement obtained after the MPC for 27 µJ input energy are presented in Fig. 3. The spectrum

Optics EXPRESS

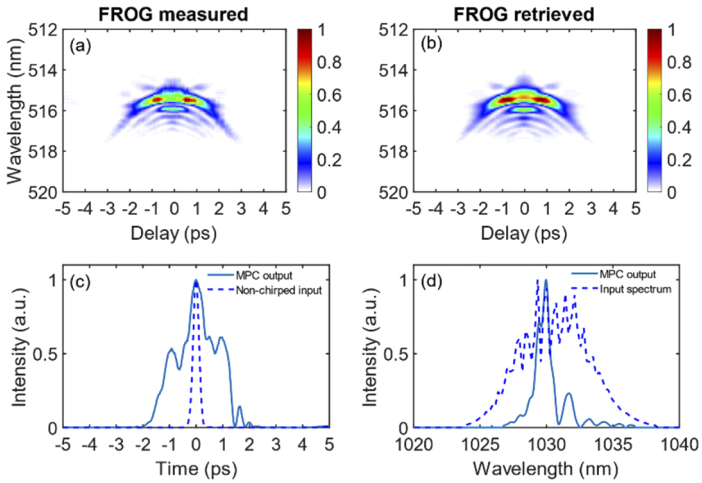

Fig. 2. (a) Measured and (b) retrieved FROG traces plotted in linear scale at the MPC output at 19 μJ input energy; (c) FROG-retrieved temporal intensity profile (solid) at the MPC output and the temporal profile of the input laser pulse before negative chirping (dashed); (d) FROG-retrieved spectral intensity profile (solid) at the MPC output and spectrum of the input laser pulse (dashed).

is compressed to 1.13 nm and the temporal duration is 2.1 ps at FWHM with a TBP of 0.68. Although the compressed spectral width is approximately equal to that obtained in the previous case, the spectral compression is now symmetric. This equally distributed intensity can also be seen in the FROG traces in Figs. 3(a)–3(b). Further improvement in the output spectrum, in particular lower sidelobes intensity, could be obtained by using a parabolic-shaped input pulse such as in [1,21]. The obtained temporal pulse profile approaches a square distribution, as already suggested in [22].

We now compare these experimental results to numerical simulations using a simplified model as described in [23]. This hybrid model uses a standard approach based on a generalized nonlinear Schrödinger equation in the time domain, coupled to a simple Gaussian beam evolution based on ABCD matrices that include the Kerr lens. In particular, it allows to describe the impact of nonlinearity on the beam caustic inside the MPC. The parameters used in the simulations are the same as in the experiment. The initial condition is taken from the measured input FROG traces in both cases: negative chirp introduced using the grating pair or using the pulse shaper. Figure 4 shows the temporal profiles measured at the input of the MPC along with measured and simulated spectral and temporal profiles at the output of the MPC in both experimental configurations. For the gratings compressor-induced chirp case, the estimated B-integral for the first roundtrip is 0.51 rad, while it is 0.54 rad for the second experiment, leading to a total accumulated B-integral of respectively 9.0 rad and 9.5 rad after 24 roundtrips. There is a good qualitative agreement between experimental and numerical results. In particular, we see that the change of sign for the third order spectral phase introduced by the pulse shaper leads to a change in the input intensity profile, with a steepest edge being transferred from the leading edge to the trailing edge, resulting in a more symmetric spectrally compressed spectrum.

Another critical aspect to investigate at the output of MPCs is the spatio-spectral properties. We study the spatio-spectral homogeneity of the beam after the multipass cell by using an imaging spectrometer setup. It consists of an f-f arrangement composed of an 800 lines/mm grating, a 50 mm focal length cylindrical lens and a CCD camera with a 4 μm pixel size. We also measure the beam spatial profile and M^2 quality factor at the output of the MPC. The results are presented

Optics EXPRESS

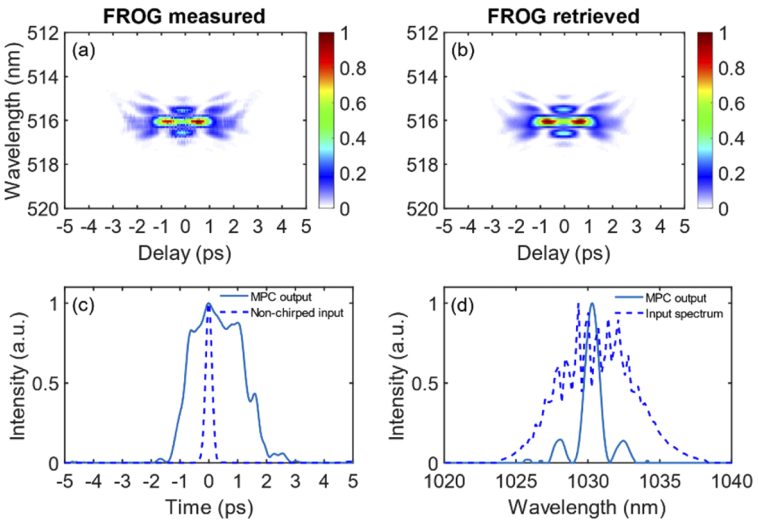

Fig. 3. (a) Measured and (b) retrieved FROG traces plotted in linear scale at the MPC output at 27 μJ input energy; (c) FROG-retrieved temporal intensity profile (solid) at the MPC output and the temporal profile of the input laser pulse before negative chirping (dashed); (d) FROG -retrieved spectral intensity profile (solid) at the MPC output and spectrum of the input laser pulse (dashed).

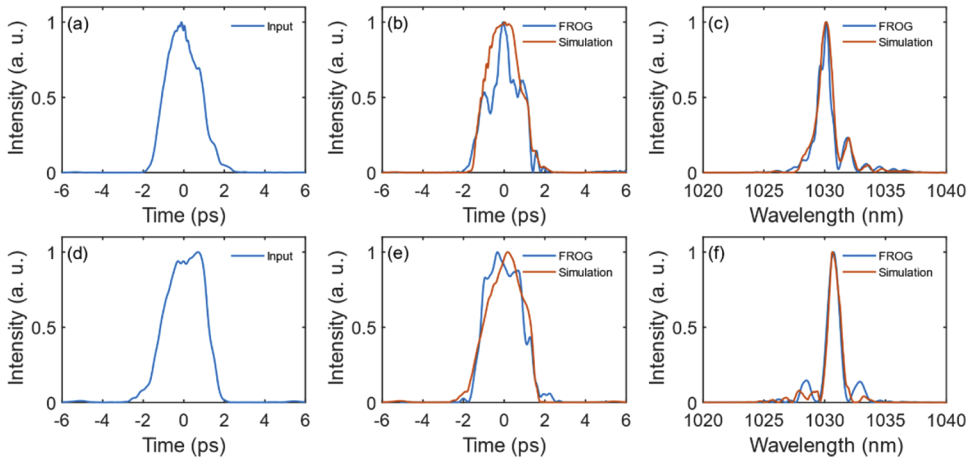

Fig. 4. First row, grating pair-induced negative chirp configuration; second row, pulse shaper-induced negative chirp configuration. (a),(d) FROG-retrieved temporal intensity profile of the input chirped pulse; (b),(e) FROG-retrieved temporal intensity profile (blue) compared to numerically simulated temporal intensity profile (red) at the MPC output; (c),(f) FROG-retrieved spectral intensity profile at the MPC output (blue) compared to spectral intensity profile obtained by simulation (red).

Optics EXPRESS

in Fig. 5. Although the intensity profile shows some degradation at the output, the measured M^2 is 1.2 × 1.0 along the vertical and the horizontal directions respectively, showing that the beam remains close to Gaussian. The larger beam size at the output of the MPC is due to the fact that the beam was collimated with a larger focal length than at the input. The mean spectral overlap factor V [24] is 98%, confirming quantitatively the absence of spatio-spectral intensity inhomogeneity.

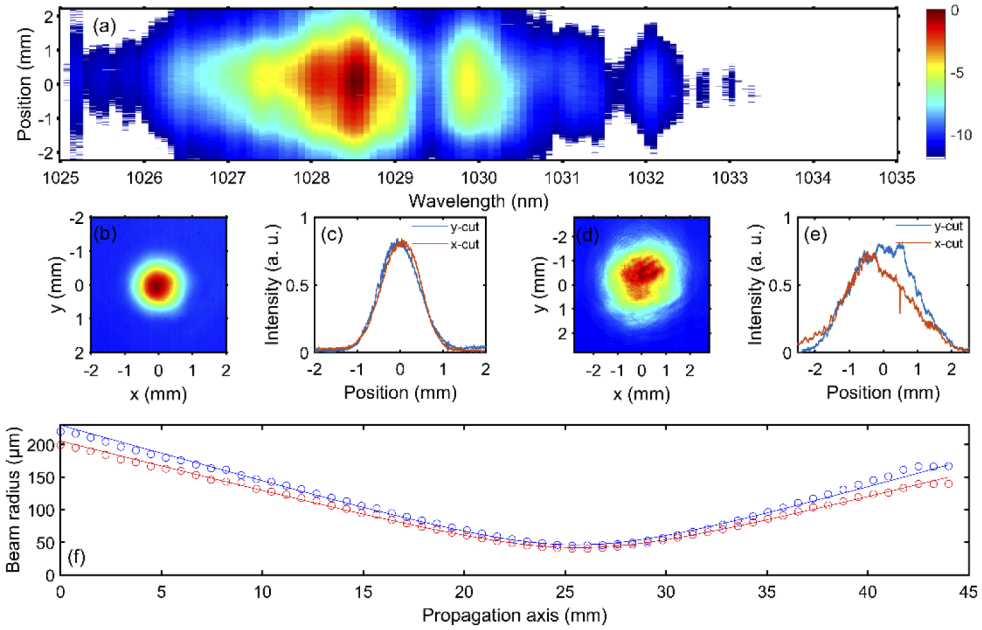

Fig. 5. (a) Experimental spectro-imaging measurement in logarithmic (dB) scale for 19 μJ input energy; (b) measured spatial beam profile of the input laser beam, and (c) corresponding lineouts; (d) measured spatial beam profile at the MPC output at 19 μJ input energy and (e) corresponding lineouts; (f) measured beam caustics and corresponding Gaussian beam fit at the MPC output in both directions.

3. Conclusion

To conclude, we report the use of a solid-state material-based MPC to implement spectral compression. This allows the generation of near-transform-limited 2.1 ps pulses from a femtosecond Yb-doped laser amplifier while preserving the spatial quality of the beam. By fine adjustments of the spectral phase at the input of the MPC using a pulse shaper, we generate a symmetric spectrum at the output. The experimentally observed temporal and spectral profiles are in good agreement with those obtained by numerical 1D simulation. We therefore demonstrate the ability to use multipass cells to perform spectral compression at energy levels beyond what is possible in fibers, extending the possibilities to design multiple output femtosecond / picosecond synchronized laser sources. Bulk-based MPCs have been demonstrated with input peak-power ten times higher to the critical peak-power [13,14]. Thus, straightforward energy scaling of such setup to 100 μJ is possible, while the mJ energy range would be accessible using gas-filled schemes.

Optics EXPRESS

Funding

Agence Nationale de la Recherche (ANR-10-LABX-0039-PALM, ANR-16-CE30-0027-01-HELLIX).

Disclosures

The authors declare no conflicts of interest.

References

1. E. R. Andresen, J. M. Dudley, D. Oron, C. Finot, and H. Rigneault, "Transform-limited spectral compression by self-phase modulation of amplitude-shaped pulses with negative chirp," Opt. Lett. **36**(5), 707–709 (2011).
2. C. W. Freudiger, W. Min, B. G. Saar, S. Lu, G. R. Holtom, C. He, J. C. Tsai, J. X. Kang, and X. Sunney Xie, "Label-Free Biomedical Imaging with High Sensitivity by Stimulated Raman Scattering Microscopy," Science **322**(5909), 1857–1861 (2008).
3. I. Will, H. I. Templin, S. Schreiber, and W. Sandner, "Photoinjector drive laser of the FLASH FEL," Opt. Express **19**(24), 23770–23781 (2011).
4. B. R. Washburn, J. A. Buck, and S. E. Ralph, "Transform-limited spectral compression due to self-phase modulation in fibers," Opt. Lett. **25**(7), 445–447 (2000).
5. L. Lavenu, M. Natile, F. Guichard, X. Délen, M. Hanna, Y. Zaouter, and P. Georges, "High-power two-cycle ultrafast source based on hybrid nonlinear compression," Opt. Express **27**(3), 1958–1967 (2019).
6. S. A. Planas, N. L. Pires Mansur, C. H. Brito Cruz, and H. L. Fragnito, "Spectral narrowing in the propagation of chirped pulses in single-mode fibers," Opt. Lett. **18**(9), 699–701 (1993).
7. Y. Zaouter, E. Cormier, P. Rigail, C. Hönninger, and E. Mottay, "30W, 10 µJ, 10-ps SPM-induced spectrally compressed pulse generation in a low non-linearity ytterbium-doped rod-type fibre amplifier," Proc. SPIE **6453**, 64530O (2007).
8. J. Limpert, T. Gabler, A. Liem, H. Zellmer, and A. Tünnermann, "SPM-induced spectral compression of picosecond pulses in a single-mode Yb-doped fiber amplifier," Appl. Phys. B **74**(2), 191–195 (2002).
9. E. R. Andresen, J. Thøgersen, and S. R. Keiding, "Spectral compression of femtosecond pulses in photonic crystal fibers," Opt. Lett. **30**(15), 2025–2027 (2005).
10. J. Pouysegur, F. Guichard, Y. Zaouter, M. Hanna, F. Druon, C. Hönninger, E. Mottay, and P. Georges, "Hybrid high-energy high-power pulsewidth-tunable picosecond source," Opt. Lett. **40**(22), 5184–5187 (2015).
11. A. V. Mitrofanov, M. M. Nazarov, A. A. Voronin, D. A. Sidorov-Biryukov, V. Y. Panchenko, and A. M. Zheltikov, "Free-beam spectral self-compression at supercritical peak powers," Opt. Lett. **43**(22), 5693–5696 (2018).
12. J. Liu, X. Chen, J. Liu, Y. Zhu, Y. Leng, J. Dai, R. Li, and Z. Xu, "Spectrum reshaping and pulse self-compression in normally dispersive media with negatively chirped femtosecond pulses," Opt. Express **14**(2), 979–987 (2006).
13. J. Schulte, T. Sartorius, J. Weitenberg, A. Vernaleken, and P. Russbueldt, "Nonlinear pulse compression in a multi-pass cell," Opt. Lett. **41**(19), 4511–4514 (2016).
14. J. Weitenberg, T. Saule, J. Schulte, and P. Rußbüldt, "Nonlinear Pulse Compression to Sub-40 fs at 4.5 µJ Pulse Energy by Multi-Pass-Cell Spectral Broadening," IEEE J. Quantum Electron. **53**(6), 1–4 (2017).
15. M. Ueffing, S. Reiger, M. Kaumanns, V. Pervak, M. Trubetskov, T. Nubbemeyer, and F. Krausz, "Nonlinear pulse compression in a gas-filled multipass cell," Opt. Lett. **43**(9), 2070–2073 (2018).
16. L. Lavenu, M. Natile, F. Guichard, Y. Zaouter, X. Delen, M. Hanna, E. Mottay, and P. Georges, "Nonlinear pulse compression based on a gas-filled multipass cell," Opt. Lett. **43**(10), 2252–2255 (2018).
17. M. Kaumanns, V. Pervak, D. Kormin, V. Leshchenko, A. Kessel, M. Ueffing, Y. Chen, and T. Nubbemeyer, "Multipass spectral broadening of 18 mJ pulses compressible from 1.3 ps to 41 fs," Opt. Lett. **43**(23), 5877–5880 (2018).
18. L. Lavenu, M. Natile, F. Guichard, Y. Zaouter, M. Hanna, E. Mottay, and P. Georges, "High-energy few-cycle Yb-doped fiber amplifier source based on a single nonlinear compression stage," Opt. Express **25**(7), 7530–7537 (2017).
19. D. Herriott, H. Kogelnick, and R. Kompfner, "Off-axis paths in spherical mirror interferometers," Appl. Opt. **3**(4), 523–526 (1964).
20. P. Kabaciński, T. M. Kardaś, Y. Stepanenko, and C. Radzewicz, "Nonlinear refractive index measurement by SPM-induced phase regression," Opt. Express **27**(8), 11018–11028 (2019).
21. J. Fatome, B. Kibler, E. R. Andresen, H. Rigneault, and C. Finot, "All-fiber spectral compression of picosecond pulses at telecommunication wavelength enhanced by amplitude shaping," Appl. Opt. **51**(19), 4547–4553 (2012).
22. C. Finot and S. Boscolo, "Design rules for nonlinear spectral compression in optical fibers," J. Opt. Soc. Am. B **33**(4), 760–767 (2016).
23. M. Hanna, N. Daher, F. Guichard, X. Delen, and P. Georges, "Hybrid pulse propagation model and quasi-phase matched four-wave mixing in multipass cells," submitted for publication.
24. J. Weitenberg, A. Vernaleken, J. Schulte, A. Ozawa, T. Sartorius, V. Pervak, H. Hoffmann, T. Udem, P. Russbüldt, and T. W. Hänsch, "Multi-pass-cell-based nonlinear pulse compression to 115 fs at 7.5 µJ pulse energy and 300 W average power," Opt. Express **25**(17), 20502–20510 (2017).